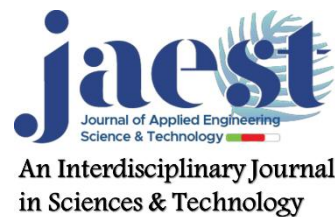


Issues lists available at **UMKB journals**

Journal of Applied Engineering Science & Technology

Journal home page: <https://journals.univ-biskra.dz/index.php/jaest><https://doi.org/10.69717/jaest.v5.i1.108>

Corrosion inhibition effect of arabic gum on Cu-WC nanocomposite coating synthesized by electrodeposition technology

Hachemi Ben Temam^{1,*}, Madjeda Zarour², Bacha Oussama³, Elhachmi Guettaf Temam¹, Amer Mekkaoui¹¹ Physics laboratory of Thin Layers and Applications, Biskra University, BP 145 RP, Biskra 07000, Algeria² Industrial chemistry department, Biskra University, BP 145 RP, Biskra 07000, Algeria³ Laboratory of Dynamic Interactions and Reactivity of Systems, Kasdi Merbah University, Ouargla 30000, Algeria

ABSTRACT

Nanostructured Cu-WC composite coatings were electrodeposited by co-deposition process onto pretreated steel substrate from an acidic sulfate electrolyte bath containing various amount of dispersed WC powder. The analysis by scanning electron microscopy shows those Cu-WC composite coatings containing cracks and random distribution of the oval-shaped WC particles. The X-ray diffraction (XRD) reveals that the structure of Cu-WC coatings is controlled by the WC powder amounts in the electrolyte baths. The average crystallite size was calculated by use X-ray diffraction analysis and its increasing is proportional to the enhancement of WC solid particles amount. The crystallite structure was fcc for electrodeposited Cu-WC nanocomposite coatings. The potentiodynamic polarization and electrochemical impedance spectroscopic studies reveal that grain refinement offers the best corrosion resistance. Arabic gum shows that it is an anodic inhibitor with high inhibitor efficiency reaches 70.95%. IR spectroscopy analysis shows several functional groups responsible for high inhibitor efficiency.

KEYWORDS

Ni-WC composite coatings
Grain size
Corrosion resistance
EIS
Arabic gum
Anodic inhibitor

ARTICLE HISTORY

Received	Revised	Accepted	Published
20 Oct 2024	05 Dec 2024	23 Dec 2024	07 Apr 2025

1 Introduction

Corrosion affects all the engineer's achievements: energy production, civil engineering, transport, machinery, medical materials, micro-electronic components, etc [1–7]. Corrosion protection consists of several actions, namely: the right choice of materials [8–10], the right shape of the parts, the addition of inhibitors to the aggressive medium [11,12], the use of coatings, electrochemical protection [13], etc.

Electrodeposition of composite coatings is one of the protective processes, most widespread against corrosion thanks to the special properties conferred on them by the incorporation of solid particles which are prepared by electrolytic co-deposition [14,15]. In recent years, the electrodeposition method has been used more and more because it has certain advantages. It is more economical in terms of materials and equipment, and also simple to use and allows creating large surfaces of geometric shapes complex [16].

A characteristic feature of these studies is drawing attention to the composite coatings based on a metallic matrix. They have several functional characteristics, including good abrasion resistance, good lubricating properties, increased hardness, good corrosion resistance and high catalytic activity in the selected electrode process [16]. The copper is a malleable and ductile metal with excellent electrical conductivity and finds extensive use as an electrical conductor and heat, as a building material, as well as a component of

different alloys [15,17–24]. The electrodeposition of Cu/solid particles composite coatings have been extensively studied by various morphological characteristics, electrical properties and corrosion resistance, but less attention was paid to their mechanical behaviour and its relationship with electrodeposition parameters [25–27]. A variety of composite coatings with different characteristics can be made, allowing the mechanical properties of coatings to be adapted for specific applications [14].

Hydrogen production, storage and use in an economical way to take on the utmost importance to many researchers. Its production projects are funded by many countries to use it as an alternative and clean energy. Numerous researches have clarified the main challenges of the H₂ industry to facilitate its use as alternative energy to fossil fuels [28,29]. The hydrogen evolution reaction (HER) is very important and has been studied in a wide range of aggressive media and electrode materials [30]. Iron metal (Cu, Ni, etc) alloys with incorporated solid particles are used as electrode materials and characterized by catalytic properties during various electrochemical processes, including hydrogen evolution process.

This work aims to investigate the effect of tungsten carbide amount in the electrolyte baths on morphology, structure and electrochemical properties as well as hydrogen evolution reaction (HER) using potentiodynamic polarization and electrochemical impedance spectroscopy methods. In addition, the effect of Arabic gum

* Corresponding author. Hachemi Ben Temam (H. Ben Temam)
E-mail : h.bentemam@univ-biskra.dz

as an inhibitor on the hydrogen evolution of Cu-WC as cathode in 3.5 % NaCl corrosion medium has been studied.

2 Experimental

2.1 Preparation of Cu-WC coatings

This study involves the electrodeposition and characterization of Cu/WC composite coatings electrodeposited on pretreated steel substrates (P265NB) to investigate the effect of tungsten carbide amount on the properties of developed deposits. This study led us to optimize the various electrodeposition parameters, namely: current density, temperature, stirring speed and the deposition time. The characterization of these developed composite coatings, therefore, requires appropriate analytical methods for each of these properties.

To guarantee the enrichment of electrolytic baths by copper ions, and to the homogeneity of deposits, we used rectangular plates of pure copper (99.99%) as anodes, whereas steel substrates were used as cathode. Before deposition, the substrates have to be degreased electrolytically in 50 g/l Na₂CO₃ + 15 g/l NaOH solution for 3 min at 2 A/dm² to remove oil and greases, then pickled in 10% HCl solution to remove oxide traces [31].

Electrodeposition was carried out at an ambient temperature from economic and strong acidic sulfate electrolyte baths (pH=1), containing CuSO₄·5H₂O-80g/l and H₂SO₄-20g/l, whereas, the concentration of WC particles ranged from 5 to 25 g/l (Table 1). The electroplating time and current density are fixed at 30 min and 5 A/dm², respectively.

Table 1. Bath composition and deposition conditions for Cu-WC composite coatings.

Compositions (g/l)	CuSO ₄ ·5H ₂ O	80
	H ₂ SO ₄	20
	WC powder	5, 10, 15, 20 and 25
Conditions	Current density (mA/cm ²)	50
	pH	1
	Time (min)	30
	Temperature (°C)	25

2.2 Characterization of Cu-WC coatings

The morphology of Cu-WC composite coatings was investigated using a JSM-6390 Lv scanning electron microscopy (SEM). Structural investigations and phase composition were conducted by the XRD method using a Bruker diffractometer (D8 Advance model) with Cu K α -radiation (1.5406 Å). The mean crystal sizes were determined from the peak width using Scherrer's equation modified by Warren and Biscoe [27,31,32]:

$$\tau = \frac{0,94 \cdot \lambda}{\beta \cdot \cos\theta} \quad (1)$$

Where, θ is the position of the peak in the diffractogram, β is the integral peak broadening (in radians) which is approximately the full width at half maximum (FWHM) value, λ is the wavelength (in Å), and is the grain size. For estimating the crystal size, an average value is considered to be FWHM (or β).

To study the electrocatalytic properties as well as the hydrogen evolution reaction (HER) of Cu-WC composite coatings, the samples were immersed in 3.5 % NaCl and 3.5 % NaCl + 0.5 g/l Arabic gum corrosion media for 1h. Potentiodynamic polarization measurements were conducted at a scanning rate of 0.5 mV/s by using a standard three-electrode cell with the coated sample as a working electrode, Pt as the auxiliary electrode and saturated calomel electrode as a reference electrode. The corrosion potential (E_{corr}) or corrosion current (i_{corr}) for the specimens was determined by calculating the cathode and anode Tafel curves provided by Volta Master 4 software.

The HER activity of resulting Cu-WC coatings was also evaluated in 3.5 % NaCl and 3.5 % NaCl + 0.5 g/l Arabic gum corrosion media for 1h by impedance (EIS) method, which is carried out using a device model (Potentiostat/Galvanostat PGZ 301) and a frequency range between 10 kHz and 50 mHz. To satisfy the linearity condition of the response of the electrochemical system studied, the amplitude of the disturbance voltage (ΔE) must be quite low: for all experiments, a value of 10 mV was fixed. The EIS plots are fitted using EC-Lab software.

IR spectroscopy is one of the most effective methods for identifying organic and inorganic molecules from their vibrational properties. To study the different functions of the organic inhibitor using FTIR technique, the powder (Arabic gum) was analyzed in comparison with KBr (reference element), in order to know the effective functional groups attributed to the inhibitor efficiency.

3 Results and Discussion

The morphology of Cu-WC composite coatings electrodeposited at various WC powder amount is shown in Fig. 1. It is obvious that the presence of WC solid particles incorporated into the copper matrix significantly widens the actual surface of the composite coatings. The observation of the different deposits by scanning electron microscopy leads us to say that these composite Cu-WC coatings are heterogeneous, compact and have some cracks due to internal stresses caused by the intensification of the hydrogen reaction (HER). The effect of the WC powder amount on Cu-WC coatings morphology is clearly observed by the increase of oval-shaped WC solid particles incorporated into the copper matrix as the WC amount increases (Fig.1). In addition, we observe that WC particles are randomly distributed in the surface of the deposit, possibly due to the effect of hydrogen bubbles form on the surface of the samples under the influence of baths acidity.

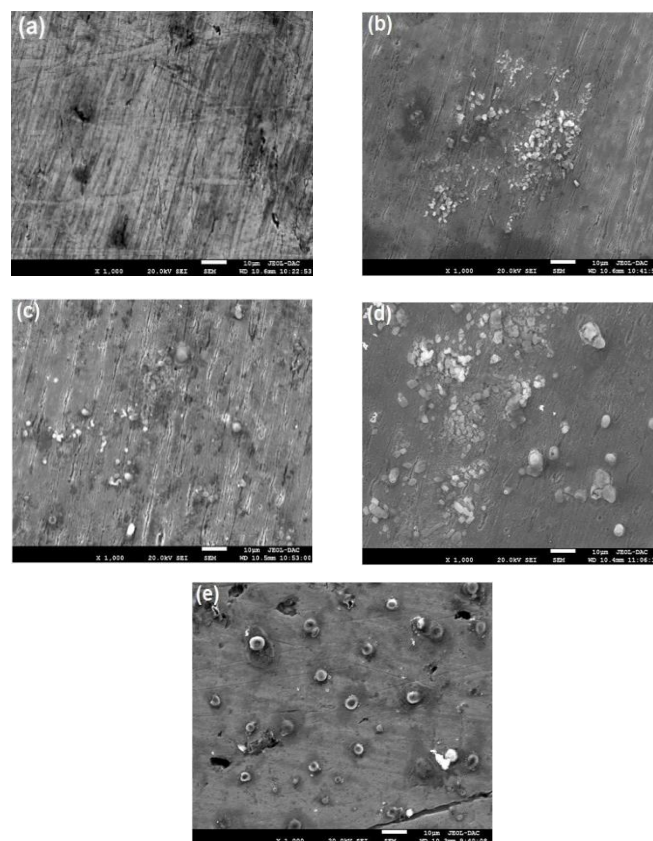


Fig.1. XRD patterns of Cu-WC composite coatings electrodeposited at different amount of WC powder.

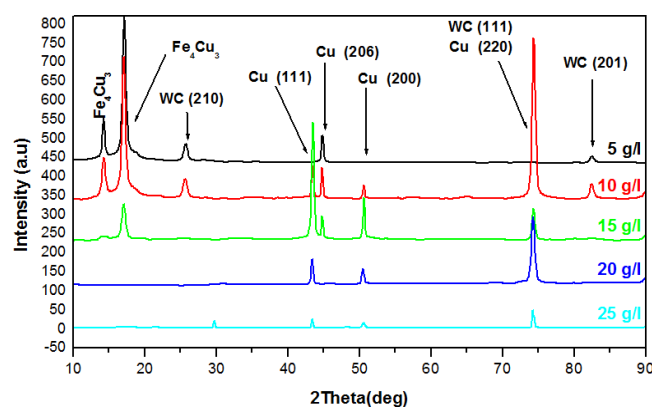


Fig.2. SEM images of Cu-WC composite coatings electrodeposited at various amount of WC particles: (a) 5g/l, (b) 10g/l, (c) 15 g/l, (d) 20g/l, (e) 25g/l.

XRD patterns of Cu-WC composite coatings were treated by X'pert high score plus software, based on PDF4 file to reveals the phases. Fig. 2 shows that the structure is well crystalline and all the peaks are well resolved. It can be seen that the preferential plane is influenced by tungsten carbide amount, these [(1 1 1) and (2 2 0)] planes are relative to the cubic Cu phase (ASTM reference code 00.003.1018). At the concentrations 5, 10 and

15g/l of WC powder, XRD patterns reveals the WC phase at 2theta: 25-26°, 45-46° and 82-83° corresponding to the following planes: (2 1 0), (2 0 6) and (4 4 4), respectively; (ASTM reference code 00.020.1314). At 5 and 10 g/l concentrations of WC, we observe the presence of undesirable peaks which are the most intense relative to the Fe₃Cu₃ phase (ASTM reference code 00.042.1067). This can be explained by the fact that the reduction of Cu and Fe cations is more favorable than the incorporation of WC particles. This phenomenon is reduced to the oxidation of steel substrates under the effect of high electrolyte baths acidity (pH=1). In addition, Fe₃Cu₃ phase is formed at low concentration of WC solid particles in the electrolytic baths, thanks to the richness of the interface substrates-electrolyte by the electrons under the effect of applied current density and the high overvoltage of hydrogen on Fe. Based on the above, we can conclude that the low amount WC particles leads to its poor distribution and the low development of the crystalline structure subjected to convective movements by Cu²⁺ cations; which implies the low incorporation of WC by the charge transfer reaction at the cathode.

The effect of WC amount on the grain size of Cu-WC composite coatings is shown in Fig. 3. It is observed that the increase of the grain size is proportional to the enhancement of WC solid particles amount in the electrolytic baths. This result is associated with the reduction of the main peak intensity with the increase of the WC particles amount (Table 4).

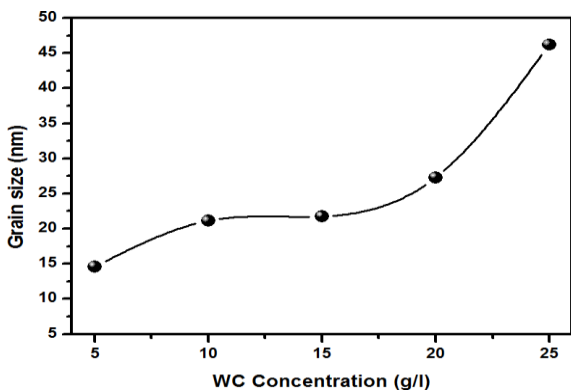


Fig.3. Grains size of Cu-WC composite coatings electrodeposited at different amount of WC powder.

Fig. 4 presents the potentiodynamic polarization plots of the Cu-WC nanocomposites coatings immersed in 3.5% NaCl and NaCl+0.5 g/l Arabic gum solutions for 1 h at ambient temperature. Table 2 and 3 portrayed the electrochemical kinetic parameters which are determined from the intersection of the anodic and cathodic Tafel lines extrapolation. The inhibitory efficiency was estimated from the following equation [33]:

$$\epsilon\% = \frac{i_{corr}^{inh} - i_{corr}}{i_{corr}^{inh}} \cdot 100 \quad (2)$$

$i_{corr}^{inh} - i_{corr}$, are the corrosion current densities with and without using the inhibitor, respectively.

Table 2. Results of polarization measurements for Cu-WC coatings in 3.5% NaCl solution.

Parameters	WC Concentrations (g/l)				
	5	10	15	20	25
E _{corr} (mV)	-523.3	-463.3	-487.7	-548.5	-243.6
i _{corr} (μA/cm ²)	29.6	25.17	101.4	124.7	145.6
β _a (mV)	214.9	144.5	154.0	373.0	318.7
β _c (mV)	-182.5	-195.0	-191.9	-204.2	-561.5
R _p (ohm.cm ²)	1010	1030	250.2	543.2	495.6
Corrosion rate (μm/Y)	346.2	294.4	1185	1458	1703

The resulting Tafel plots displayed the highest corrosive resistance (1030 ohm.cm²), and the lowest corrosion current density for Cu-WC nanocomposite coatings synthesized at 10 g/l of WC (Table 2). Furthermore, the corrosion rate (294.4 μm/y) of this sample is lower than for the other types. It is evident that the corrosion current density values are disproportionate to the grain size. It is well-known that grain refinement leads to improvements in corrosion resistance. Ralston and Birbilis [34] explained that the existing literature is often contradictory, even within the same alloy class, and a coherent understanding of how grain size influences corrosion response is largely lacking. Srikant Gollapudi [35] has suggested that the broader grain size distribution leads to higher corrosion resistance in the active environment whilst the broader grain size distribution leads to lower corrosion resistance in the passivating environment. [36] et al. have also

suggested that linear polarization resistance (R_p) showed a clear trend of increasing R_p value with grain refinement. The main results of Ben-Hamu et al. [37] show that when zirconium is added to refine the grain size, the corrosion resistance of the alloy is significantly improved. Based on the above, the corrosion current density values for copper layers do not match the aforementioned hypotheses. Therefore, we believe that the corrosion resistance is not affected only by the grains size of the surface, as this hypothesis is valid only in the case of uniform distribution and complete coverage of the surface by the grains, which implies that if the surface contains pores or cracks as is the example in this study, the resistance corrosion is subject to several combined factors. In general, we observe the increase in corrosion current density values with the increase of the amount of toilet in electrolyte baths, but not gradually as well as the grain size. The corrosion current density of the working electrode in 3.5% NaCl is equal to 29.6 μA/cm². After the injection of the inhibitor (Arabic gum) in the same condition as the test without inhibitor (T = 25 ° C, immersion time = 1h to allow the formation of the protective film), the measurement of i_{corr} gives the value 11.94 μA/cm². According to the traces of Fig. 4, we can say that the inhibitor has an anodic behaviour, which implies that i_{corr} tends towards less positive values, therefore it becomes ennobled. Moreover, the inhibitor efficiency values are divergent and varied according to the type of investigated samples, which means that the surface morphology and microstructure have an effect on the function of Arabic gum. The inhibitor efficiency reaches a maximum value of 62.39% according to the sample synthesized at 25g/l of WC powder (Table 3).

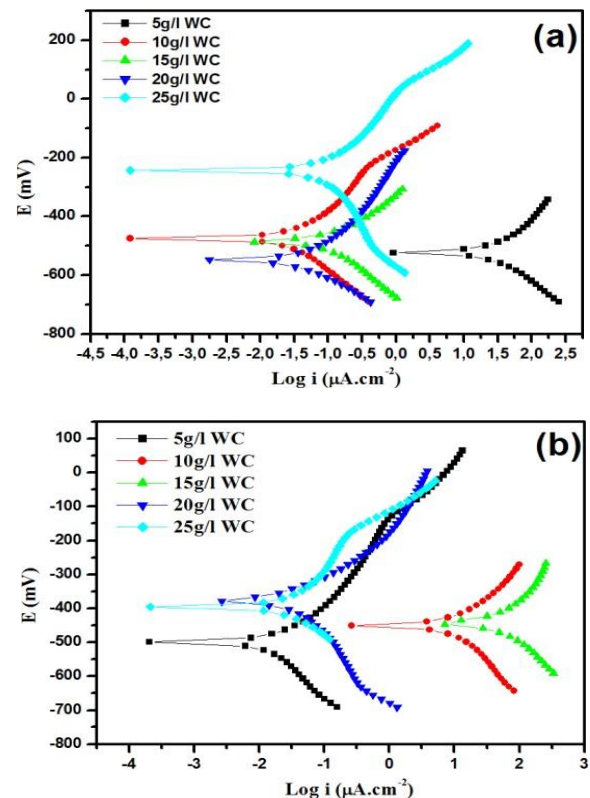


Fig.4. Polarization curves of Cu-WC composite coatings electrodeposited at different amount of WC powder.

Table 3. Results of polarization measurements for Cu-WC coatings in 3.5% NaCl + 0.5 g/l arabic gum solution.

Parameters	WC Concentrations (g/l)				
	5	10	15	20	25
E _{corr} (mV)	-536.6	-451.3	-442.5	-379.2	-384.2
i _{corr} (μA/cm ²)	15.9	11.94	59.09	61.5	-384.2
β _a (mV)	189.1	182.7	242.2	165.7	54.76
β _c (mV)	-169.1	-240.9	-198.2	-335.9	400.9
R _p (ohm.cm ²)	1370	2770	583.6	768.2	-255.7
Corrosion rate (μm/Y)	185.7	139.6	691.1	719.3	1160

Fig. 5 illustrates the EIS analysis (Nyquist diagrams) of Cu-WC composite coatings immersed in 3.5% NaCl and 3.5% NaCl+0.5 g/l Arabic gum solutions for 1 h. The inhibitory efficiency was estimated from the following equation [33]:

$$\epsilon\% = \frac{R_{ct}^{inh} - R_{ct}}{R_{ct}^{inh}} \cdot 100 \quad (3)$$

R_{ct}^{inh} and R_{ct} is the charge transfer resistance with and without using inhibitor, respectively.

At high frequency, the electrolyte resistance (R_s) was determined by the intersection with the abscissa axis and referred to the resistance between the Cu-WC electrode and reference electrode. At low frequency, the capacitive loop is associated with the charge transfer resistance (R_{ct}) in parallel with the double layer capacity (C_{dl}), which is attributed to the electrochemical reaction. This type of measurement makes it possible to study the global electrocatalytic reactivity of Cu-WC electrodes, as well as to highlight the distributions of time constants which can usually be described by constant phase elements (CPE) [38–40]. The resistance of the solution is low, which implies that the medium is a good conductor. The lowest value is recorded at the amount of 5 g/l of tungsten carbide (Table 4).

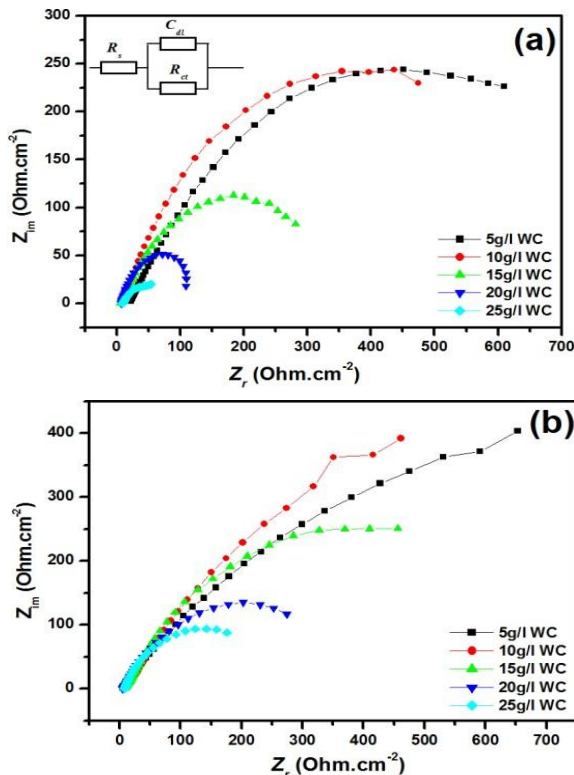


Fig.5. Nyquist diagrams of Cu-WC composite coatings immersed in (a) 3.5 % NaCl and (b) NaCl+0.5 g/l Arabic gum solutions for 1 h.

Fig. 5 shows that each spectrum having a single time constant at high frequency (HF) of the semicircle. The low frequency is attributed to the electrochemical reaction and indicates (R_{ct}) the charge transfer resistance of the (HER) hydrogen evolution reaction. Nanocomposite Cu-WC prepared at 5g/l of WC obtained the maximum impedance value among all specimens, implying it possesses the optimal anti-corrosion ability. (R_{ct}) presents a very important value (882.9 ohm.cm²) for the samples synthesized at 5g/l of WC. It's clear demonstrated that R_{ct} values maintained the same order after increasing the organic inhibitor. In addition, R_{ct} of all the electrodes depends on both the grain size and the presence of the inhibitor, where their presence increases the values of R_{ct} and consequently its efficiency reaches a maximum value of 70.95% for the deposit prepared at 25g/l of WC, which is due to the random distribution of the oval-shaped gains compared to the other samples (Fig. 5). These results are consistent with the potentiodynamic polarization analysis results.

Table 4. Fitted EIS parameters for Cu-WC composite coatings in 3.5% NaCl solution.

Parameters	WC Concentrations (g/l)				
	5	10	15	20	25
Rs (ohm/cm²)	21.82	9.613	6.608	7.446	8.998
Rct (ohm/cm²)	882.9	747.8	390.0	138.0	78.12
Cdl (μF/cm²)	180.2	425.6	1632	5762	6437
Grains size (nm)	14.6	21.12	21.75	27.29	46.18

In the absence of a response related to the adsorption of hydrogen, the Randles model of the equivalent electrical circuit is the most used to explain the HER on the Cu-based electrode. We find a phase shift with respect to the real axis, Fig. 5, which can be explained by the heterogeneity of the surface. This is a constant phase element (CPE) which realizes surface heterogeneities. The EIS plots shown in Fig. 5 are analyzed using

one time-constant electrochemical equivalent circuit (EEC) model and fitted through EC-Lab software (Fig. 6a). The represented elements that have shown in the circuit are R_s (solution resistance), R_{ct} (charge transfer resistance of the electrode reactions) and C_{dl} representing the double layer capacitance between the solution and the composite coating. The fitted parameters have been shown in (Tables 4 and 5).

Table 5. Fitted EIS parameters for Cu-WC composite coatings in 3.5% NaCl + 0.5 g/l Arabic gum solution.

Parameters	WC Concentrations (g/l)				
	5	10	15	20	25
Rs (ohm/cm²)	4.235	10.30	9.582	5.453	8.039
Rct (ohm/cm²)	1645	1641	835.1	438.3	268.9
Cdl (μF/cm²)	1218	969.6	602.1	3630	3740
ε (%)	46.33	54.43	53.23	68.51	70.95

Fig. 6 shows the IR spectrum of KBr and the natural powder of Arabic gum. The Arabic gum analyzed in comparison with KBr to know the effective functional groups attributed to the inhibitory effects on the electrochemical behavior of Cu-WC composite coatings. The arabic gum has several functional groups such as aldehyde compounds, ketone and also the aromatic or phenolic compounds (Table 6). All these known compounds have inhibitory properties [14].

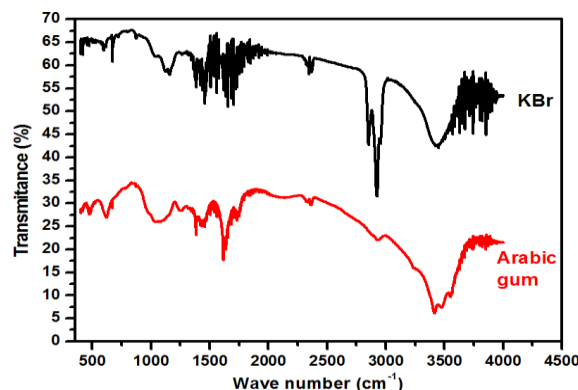


Fig.6. IR spectrum of KBr and the natural powder Arabic gum.

Table 6. Fitted EIS parameters for Cu-WC composite coatings in 3.5% NaCl solution.

Structure	Wave no. (cm ⁻¹)
(-OH)	3400
(C-H)CH ₃	2975
(-CH)C-CH ₃	1470-1435,1385-1370
(C-OH)	1000-1175
(C-O-C)	1060-1150

4 Conclusion

Nanostructured Cu-WC composite coatings with randomly particle distribution were obtained on carbon steel by electrodeposition route from acid sulfate bath containing suspended WC particles.

SEM images show that Cu-WC composite coatings containing cracks and random distribution of the oval-shaped WC particles. The structure of Cu-WC coatings and grain size is controlled by WC powder amounts in the electrolyte baths.

Corrosion studies showed that grain refinement offers the best electrochemical corrosion resistance and the highest activity in HER. The injection of Arabic gum containing several inhibitory functional groups leads to an improvement in the corrosion resistance and therefore the electrocatalytic activity of Cu-WC electrodes in 3.5% NaCl.

Declaration of Competing Interest

The authors declare that they have no known competing financial interests or personal relationships that could have appeared to influence the work reported in this paper.

References

[1] F. Zhang, P. Ju, M. Pan, D. Zhang, Y. Huang, G. Li, X. Li, Self-healing mechanisms in smart protective coatings: A review, Corros Sci 144 (2018) 74–88. <https://doi.org/10.1016/J.CORSCI.2018.08.005>.
 [2] L. Guo, S.R. Street, H.B. Mohammed-Ali, M. Ghahari, N. Mi, S. Glanvill, A. Du Plessis, C. Reinhard, T. Rayment, A.J. Davenport, The effect of relative humidity change on atmospheric pitting corrosion of stainless steel 304L, Corros Sci 150 (2019) 110–120. <https://doi.org/10.1016/J.CORSCI.2019.01.033>.

- [3] A. Marciales, Y. Peralta, T. Haile, T. Crosby, J. Wolodko, Mechanistic microbiologically influenced corrosion modeling—A review, *Corros Sci* 146 (2019) 99–111. <https://doi.org/10.1016/J.CORSCI.2018.10.004>.
- [4] B. Saadi, S. Rahmane, E.G. Temam, Structural, optical and electrical properties of spray deposited indium-doped Cr₂O₃ thin films, *Journal of Optics (India)* 53 (2024) 582–589. <https://doi.org/10.1007/s12596-023-01252-4>.
- [5] A. Mekkaoui, E.G. Temam, S. Rahmane, B. Gasmii, A New Study on the Effect of Pure Anatase TiO₂ Film Thickness on Gentian Violet Photodegradation Under Sunlight: Considering the Effect of Hole Scavengers, *Trends in Sciences* 20 (2023). <https://doi.org/10.48048/tis.2023.3766>.
- [6] K. Yousra, E. Guettaf Temam, R. Saâd, H. Barkat, Effect of film thickness on the electrical and the photocatalytic properties of ZnO nanorods grown by SILAR technique, *Phys Scr* 12 (2023). <https://doi.org/10.1088/1402-4896/ad0ae7>.
- [7] A. Mekkaoui, E.G. Temam, S. Rahmane, B. Gasmii, A New Study on the Effect of Pure Anatase TiO₂ Film Thickness on Gentian Violet Photodegradation Under Sunlight: Considering the Effect of Hole Scavengers, *Trends in Sciences* 20 (2023). <https://doi.org/10.48048/tis.2023.3766>.
- [8] B. Ferial, E.G. Temam, S. Rahmane, B. Nadjette, M. Althamthami, F. Maroua, Effect of post annealing temperature upon the electrical properties and kinetics of photocatalytic degradation by dip coated ZnO thin film, *STUDIES IN ENGINEERING AND EXACT SCIENCES* 5 (2024) e12921. <https://doi.org/10.54021/see5v5n3-123>.
- [9] M. Ferhat, H. Djemai, E. Guettaf Temam, A. Labeled, L. Lahag, Y. Sid Amer, Sustainable composite materials with date palm rachis fibers for enhanced insulation and structural integrity, *Phys Scr* 99 (2024). <https://doi.org/10.1088/1402-4896/ad69e2>.
- [10] K. Fouad, E.G. Temam, T. Adel, B.A. Errahmane, Effect of substrates on the structural and optical properties of cobalt-doped ZnO thin films, *STUDIES IN ENGINEERING AND EXACT SCIENCES* 5 (2025) e13132. <https://doi.org/10.54021/see5v5n3-144>.
- [11] R. Laamari, J. Benzakour, F. Berrekhis, A. Abouelfida, A. Derja, D. Villemin, Corrosion inhibition of carbon steel in hydrochloric acid 0.5 M by hexa methylene diamine tetramethyl-phosphonic acid, *Arabian Journal of Chemistry* 4 (2011) 271–277. <https://doi.org/10.1016/J.ARABJC.2010.06.046>.
- [12] L. Faride, B.T. Hachemi, G.T. Elhachmi, Characterization of nano-crystalline NiP alloy coatings electrodeposited at various current densities, *Iranian Journal of Materials Science and Engineering* 18 (2021). <https://doi.org/10.22068/ijmse.2237>.
- [13] M. Sabouri, T. Shahrabi, H.R. Faridi, M.G. Hosseini, Polypyrrole and polypyrrole-tungstate electropolymerization coatings on carbon steel and evaluating their corrosion protection performance via electrochemical impedance spectroscopy, *Prog Org Coat* 64 (2009) 429–434. <https://doi.org/10.1016/J.PORGCOAT.2008.08.003>.
- [14] E.G. Temam, A. Elkhanssa, H. Ben Temam, F. Kermiche, H. Benrah, The influence of Arabic gum on the catalytic properties of Ni-Mo alloy coatings to intensify hydrogen evolution reaction, *Anti-Corrosion Methods and Materials* 64 (2017) 580–587. <https://doi.org/10.1108/ACMM-10-2016-1722>.
- [15] E. Aidaoui, H. Ben Temam, O. Belahssen, E.H.G. Temam, Morphological, structural, microhardness and electrochemical characterizations of electrodeposited cr and ni-w coatings, *Acta Metallurgica Slovaca* 24 (2018) 234–240. <https://doi.org/10.12776/ams.v24i3.1105>.
- [16] B. Łosiewicz, Electrodeposition Mechanism of Composite Coatings, *Solid State Phenomena* 228 (2015) 65–78. <https://doi.org/10.4028/WWW.SCIENTIFIC.NET/SSP.228.65>.
- [17] L. Lemya, B.T. Hachemi, G.T. Elhachmi, Microstructural, surface and electrochemical properties of electrodeposited Ni-WC nanocomposites coatings, *Main Group Chemistry* 21 (2022) 763–772. <https://doi.org/10.3233/MGC-210146>.
- [18] N. Ouhabab, E.G. Temam, H. Ben Temam, A. Gana, Improvement of the microstructure and corrosion behavior of Ni-TiO₂ composite coatings electrodeposited at various amounts of TiO₂ powder, *STUDIES IN ENGINEERING AND EXACT SCIENCES* 5 (2024) e9185. <https://doi.org/10.54021/see5v5n2-336>.
- [19] H. Houada, G.T. Elhachmi, M. Althamthami, H. Ben Temam, S. Rahmane, Property Analysis of β-Tetragonal Bismite Thin Films: Varied Concentrations and Enhanced Photocatalytic Efficiency, *Iranian Journal of Materials Science and Engineering* 21 (2024) 103–118. <https://doi.org/10.22068/ijmse.3514>.
- [20] N. Mokrani, E.G. Temam, H. Ben Temam, H. Barkat, M. Althamthami, Enhancing water purification with light-activated strontium-doped ZnO thin films, *Advances in Natural Sciences: Nanoscience and Nanotechnology* 16 (2025). <https://doi.org/10.1088/2043-6262/ada005>.
- [21] N. Mokrani, E. Guettaf Temam, H. Barkat, H. Ben Temam, S. Rahmane, M. Althamthami, Boosting photocatalytic stability: hydrophilic Sr-doped ZnO thin films prepared via the SILAR method for enhanced performance over multiple cycles, *Phys Scr* 99 (2024). <https://doi.org/10.1088/1402-4896/ad6ffb>.
- [22] M. Althamthami, G.T. Elhachmi, H. Ben Temam, G.G. Hasan, S. Rahmane, B. Gasmii, Effect of different Cu:Co film concentrations on photocatalytic reactions of ethanol, MB, AMX, and Cr(VI): A study of film properties & effects of photooxidation, *J Environ Chem Eng* 11 (2023). <https://doi.org/10.1016/j.jece.2023.111247>.
- [23] M. Althamthami, H. Ben Temam, E.G. Temam, S. Rahmane, B. Gasmii, G.G. Hasan, Impact of surface topography and hydrophobicity in varied precursor concentrations of tenorite (CuO) films: a study of film properties and photocatalytic efficiency, *Sci Rep* 14 (2024). <https://doi.org/10.1038/s41598-024-58744-x>.
- [24] H. Nezzal, S. Rahmane, E.G. Temam, M. Al-Abri, H.H. Kyaw, B. Gasmii, M. Althamthami, H. Ben Temam, J. Hu, Photo-deposition of AgO thin films on TiO₂ substrate for (P-N) hetero-junction applications: Considering the degree of contamination, *J Alloys Compd* 1010 (2025). <https://doi.org/10.1016/j.jallcom.2024.177331>.
- [25] V. Medeliené, A. Kosenko, Structural and Functional Properties of Electrodeposited Copper Metal Matrix Composite Coating with Inclusions of WC, *Metals* 14 (2008) 29–33. <https://matcs.ktu.lt/index.php/MatSc/article/view/26260>.
- [26] H.B. Temam, E.G. Temam, Analysis of the co-deposition of Al₂O₃ particles with nickel by an electrolytic route: The influence of organic additives presence and Al₂O₃ concentration, in: *AIP Conf Proc*, American Institute of Physics Inc., 2016. <https://doi.org/10.1063/1.4945977>.
- [27] M. Diafi, S. Benramache, E.G. Temam, A.M. Lakhdar, B. Gasmii, Study of Zn-Ni alloy coatings modified by nano-AL₂O₃ particles incorporation, *Acta Metallurgica Slovaca* 22 (2016) 171–180. <https://doi.org/10.12776/ams.v22i3.706>.
- [28] A.M. Abdalla, S. Hossain, O.B. Nisfindy, A.T. Azad, M. Dawood, A.K. Azad, Hydrogen production, storage, transportation and key challenges with applications: A review, *Energy Convers Manag* 165 (2018) 602–627. <https://doi.org/10.1016/J.ENCONMAN.2018.03.088>.
- [29] C. Zlotea, Y. Oumellal, K. Provost, C.M. Ghimbeu, Experimental challenges in studying hydrogen absorption in ultrasmall metal nanoparticles, *Front Energy Res* 4 (2016) 205665. <https://doi.org/10.3389/FENRG.2016.00024/BIBTEX>.
- [30] G.E. Badea, I. Maior, A. Cojocar, I. Pantea, T. Badea, KINETICS OF THE HYDROGEN EVOLUTION REACTION ON 18Cr-10Ni STAINLESS STEEL IN SEAWATER. II. INFLUENCE OF TEMPERATURE, *Revue Roumaine de Chimie* 54 (2009) 55–61.
- [31] E. Guettaf Temam, H. Ben Temam, S. Benramache, Surface morphology and electrochemical characterization of electrodeposited Ni-Mo nanocomposites as cathodes for hydrogen evolution, *Chinese Physics B* 24 (2015). <https://doi.org/10.1088/1674-1056/24/10/108202>.
- [32] L.S. Sanches, S.H. Domingues, C.E.B. Marino, L.H. Mascaro, Characterisation of electrochemically deposited Ni-Mo alloy coatings, *Electrochem Commun* 6 (2004) 543–548. <https://doi.org/10.1016/J.ELECOM.2004.04.002>.
- [33] T. Hong, Y.H. Sun, W.P. Jepson, Study on corrosion inhibitor in large pipelines under multiphase flow using EIS, *Corros Sci* 44 (2002) 101–112. [https://doi.org/10.1016/S0010-938X\(01\)00052-X](https://doi.org/10.1016/S0010-938X(01)00052-X).
- [34] K.D. Ralston, N. Birbilis, Effect of Grain Size on Corrosion: A Review, *Corrosion* 66 (2010) 075005–075005–13. <https://doi.org/10.5006/1.3462912>.
- [35] S. Gollapudi, Grain size distribution effects on the corrosion behaviour of materials, *Corros Sci* 62 (2012) 90–94. <https://doi.org/10.1016/J.CORSCI.2012.04.040>.
- [36] G.R. Argade, S.K. Panigrahi, R.S. Mishra, Effects of grain size on the corrosion resistance of wrought magnesium alloys containing neodymium, *Corros Sci* 58 (2012) 145–151. <https://doi.org/10.1016/J.CORSCI.2012.01.021>.
- [37] G. Ben-Hamu, D. Eliezer, K.S. Shin, S. Cohen, The relation between microstructure and corrosion behavior of Mg–Y–RE–Zr alloys, *J Alloys Compd* 431 (2007) 269–276. <https://doi.org/10.1016/J.JALLCOM.2006.05.075>.
- [38] B. Hirschorn, M.E. Orazem, B. Tribollet, V. Vivier, I. Frateur, M. Musiani, Constant-Phase-Element Behavior Caused by Resistivity Distributions in Films: II. Applications, *J Electrochem Soc* 157 (2010) C458. <https://doi.org/10.1149/1.3499565>.
- [39] B. Hirschorn, M.E. Orazem, B. Tribollet, V. Vivier, I. Frateur, M. Musiani, Determination of effective capacitance and film thickness from constant-phase-element parameters, *Electrochim Acta* 55 (2010) 6218–6227. <https://doi.org/10.1016/J.ELECTACTA.2009.10.065>.
- [40] M. Musiani, M.E. Orazem, N. Pébère, B. Tribollet, V. Vivier, Constant-Phase-Element Behavior Caused by Coupled Resistivity and Permittivity Distributions in Films, *J Electrochem Soc* 158 (2011) C424. <https://doi.org/10.1149/2.039112JES/XML>.